Platinum−Rhenium−Mercury and Related Cluster Chemistry

Leijun Hao,[†] Jianliang Xiao,[†] Jagadese J. Vittal,[†] Richard J. Puddephatt,*[,†] Ljubica Manojlović-Muir,*[,‡] Kenneth W. Muir,[‡] and Ali Ashgar Torabi[‡]

Department of Chemistry, University of Western Ontario, London, Canada N6A 5B7, and Department of Chemistry, University of Glasgow, Glasgow G12 8QQ, Scotland

Received July 7, 1995[⊗]

The 54-electron cluster cation $[Pt_3\{ReO_3\}(\mu\text{-dppm})_3]^+$, **2**, dppm = $Ph_2PCH_2PPh_2$, reacts with CO, $P(OMe)_3$, Hg, and Tl(acac), acac = MeCOCHCOMe, by addition at the Pt_3 center to give the 56-electron cluster cations $[Pt_3\{ReO_3\}(\mu_3\text{-L})(\mu\text{-dppm})_3]^+$, L = CO (**3**), Hg (**6**), or Tl(acac) (**5**), or $[Pt_3\{ReO_3\}(L)(\mu\text{-dppm})_3]^+$ (**4**) L = $P(OMe)_3$. Oxidation of **6** in the presence of mercury and $NH_4[ReO_4]$ gives the bis(mercury) cluster $[Pt_3(\mu_3\text{-Hg})_2(\mu\text{-dppm})_3][ReO_4]_2$, **7**. The structures of **2**$[PF_6]$ [cubic, space group $Pa\bar{3}$, a = 24.495(1) Å, V = 14 697(1) Å^3, Z = 8, R = 0.0421 for 3113 reflections with $I > 2\sigma(I)$], **6**$[PF_6]\cdot 2Me_2CO$ [triclinic, space group $P\bar{1}$, a = 14.502(5) Å, b = 16.712(7) Å, c = 20.814(6) Å, α = 70.00(3)°, β = 82.52(1)°, γ = 82.39(3)°, V = 4679(3) Å^3, Z = 2, R = 0.0688 for 7227 reflections with $I > 2\sigma(I)$], and **7**$[ReO_4]_2\cdot 1.5Me_2CO$ [triclinic, space group $P\bar{1}$, a = 16.088(5) Å, b = 16.307(7) Å, c = 19.390(7) Å, α = 99.49(2)°, β = 93.70(1)°, γ = 117.30(2)°, V = 4401(4) Å^3, Z = 2, R = 0.1010 for 7931 reflections with $I > 2\sigma(I)$] have been determined. Cluster **2**, which shows exact C_3 symmetry, has a nearly tetrahedral Pt_3Re core [Pt−Pt = 2.6115(6) Å, Pt−Re = 2.7010(6) Å] while **6** [Pt−Pt = 2.617(2)−2.625(2) Å, Pt−Re = 2.770(2)−2.788(2) Å, Pt−Hg = 2.868(2)−2.976(2) Å] and **7** [Pt−Pt = 2.633(4)−2.646(4) Å, Pt−Hg = 2.754(4)−2.828(4) Å] have approximately trigonal bipyramidal Pt_3ReHg and Pt_3Hg_2 cores, respectively.

Introduction

The cluster cations $[Pt_3\{Re(CO)_3\}(\mu\text{-dppm})_3]^+$, **1**, and $[Pt_3\{ReO_3\}(\mu\text{-dppm})_3]^+$, **2**, are of interest as possible models for surface Pt−Re clusters present in bimetallic Pt−Re−Al_2O_3 catalysts, in which rhenium is in a low- and a high-oxidation state, respectively (the formal oxidation states may be considered to be Re(I) in **1** and Re(VII) in **2**).[1] Both **1** and **2** have tetrahedral Pt_3Re cores and are coordinatively unsaturated since they each have only a 54-electron count (60 valence electrons is usual in coordinatively saturated tetrahedral clusters).[1] In earlier papers, it has been shown that **2** is more reactive than **1** to ligand addition and that ligands always add to **2** at platinum but usually add to **1** at rhenium or at a Pt_2Re face.[2,3] This paper gives details of the structure of **2** and of its addition reactions with neutral ligands[2a] and reports new reactions with the unusual ligands Hg and Tl^+, giving rise to Pt_3ReHg and Pt_3ReTl clusters with trigonal bipyramidal metal cores.

Results

Reactions of $[Pt_3(ReO_3)(\mu\text{-dppm})_3][PF_6]$ with Simple Ligands. The reactions of **2** with CO and with $P(OMe)_3$ are shown in eqs 1 and 2. Carbon monoxide adds to **2** to give the

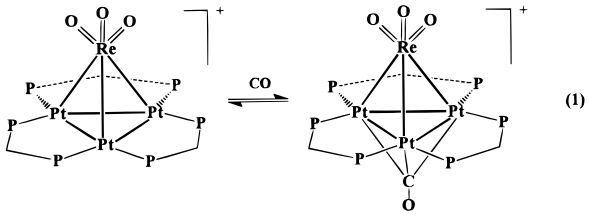

(1)

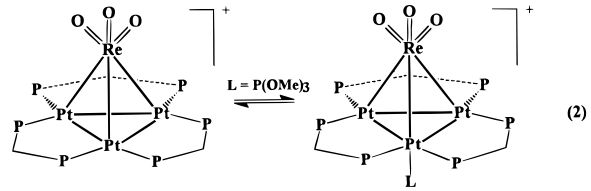

(2)

μ_3-CO complex $[Pt_3(\mu_3\text{-CO})(ReO_3)(\mu\text{-dppm})_3]^+$, **3**. The reaction was conducted in CD_2Cl_2 in an NMR tube and monitored by NMR spectroscopy. When CO was bubbled into this solution, a reaction occurred as indicated by a color change from red−brown to red, and NMR monitoring confirmed that the reaction was completed almost instantly. The reaction is easily reversible; thus bubbling N_2 through the solution resulted in the loss of CO to regenerate complex **2**, and then addition of CO regenerated **3**. Evaporation of the solvent from a solution of **3** also caused partial loss of CO and formation of **2**. Hence, **3** could not be isolated in analytically pure form, and it was characterized by IR and NMR spectroscopy in solution.

The IR spectrum of **3** in CH_2Cl_2 solution displays one terminal Re═O band with ν(Re═O) = 904 (m) cm^{-1} and one carbonyl band with stretching frequency ν(CO) = 1606 (m) cm^{-1}. The value of ν(Re═O) is the same as that of the parent cluster **2** measured in CH_2Cl_2 solution, and the value of ν(CO) is particularly low, as can be compared to ν(CO) = 1765 cm^{-1} in $[Pt_3(\mu_3\text{-CO})(\mu\text{-dppm})_3][PF_6]_2$,[4] indicating a triply bridging carbonyl with strong back-bonding.

The ^{1}H, ^{13}C, and ^{31}P NMR spectra of **3** in CD_2Cl_2 were essentially the same from room temperature to −90 °C. The

[†] University of Western Ontario.
[‡] University of Glasgow.
[⊗] Abstract published in *Advance ACS Abstracts,* December 15, 1995.

(1) (a) Xiao, J.; Vittal, J. J.; Puddephatt, R. J.; Manojlović-Muir, L.; Muir, K. W. *J. Am. Chem. Soc.* **1993**, *115*, 7882. (b) Xiao, J.; Vittal, J. J.; Puddephatt, R. J.; Manojlović-Muir, L.; Muir, K. W.; Torabi, A. A. *J. Am. Chem. Soc.* **1994**, *116*, 1129. (c) Xiao, J.; Kristof, E.; Vittal, J. J.; Puddephatt, R. J. *J. Organomet. Chem.* **1995**, *490*, 1. (d) Xiao, J.; Puddephatt, R. J. *Coord. Chem. Rev.* **1995**, *143*, 457.
(2) (a) Xiao, J.; Hao, L.; Puddephatt, R. J.; Manojlović-Muir, L.; Muir, K. W.; Torabi, A. A. *J. Chem. Soc., Chem. Commun.* **1994**, 2221. (b) Xiao, J.; Hao, L.; Puddephatt, R. J.; Manojlović-Muir, L.; Muir, K. W.; Torabi, A. A. *Organometallics* **1995**, *14*, 4183. (c) Xiao, J.; Hao, L.; Puddephatt, R. J.; Manojlović-Muir, L.; Muir, K. W.; Torabi, A. A. *Organometallics* **1995**, *14*, 2194.
(3) (a) Hao, L.; Xiao, J.; Vittal, J. J.; Puddephatt, R. J. *J. Chem. Soc., Chem. Commun.* **1994**, 2183. (b) Hao, L.; Xiao, J.; Vittal, J. J.; Puddephatt, R. J. *Angew. Chem., Int. Ed. Engl.* **1995**, *34*, 346 (c) Xiao, J.; Hao, L.; Puddephatt, R. J.; Manojlović-Muir, L.; Muir, K. W. *J. Am. Chem. Soc.* **1995**, *117*, 6316.

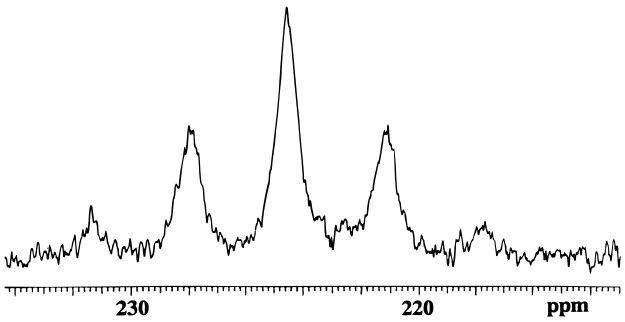

Figure 1. The ^{13}C NMR spectrum (75.46 MHz) of a ^{13}CO-enriched sample of cluster **3**. The 1:4:7:4:1 multiplet appearance is characteristic of a $Pt_3(\mu_3\text{-}CO)$ group.

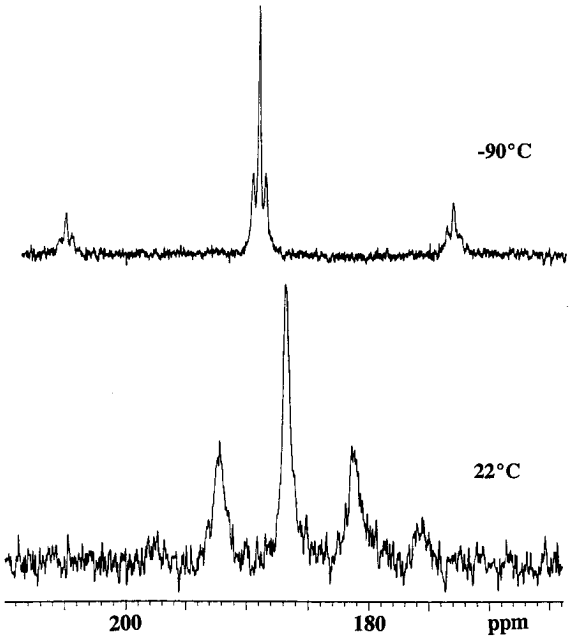

Figure 2. The ^{31}P NMR spectra (121.47 MHz) of cluster **4** at −90 °C [$^1J(PtP) = 3713$ Hz, $^2J(PtP) = 121$ Hz] and at 22 °C [$J_{av}(PtP) = 1318$ Hz].

^{31}P NMR spectrum contained only one sharp singlet resonance due to the phosphorus atoms of the dppm ligands, indicating effective C_3 symmetry. The ^{13}C NMR spectrum of a ^{13}CO-enriched sample of **3** (Figure 1) gave a resonance at $\delta(^{13}CO) = 224.6$, appearing as an apparent 1:4:7:4:1 quintet (the pattern arises from superposition of spectra from isotopomers containing one, two, and three ^{195}Pt atoms)[5] due to coupling to three equivalent platinum atoms with $^1J(PtC) = 513$ Hz. The chemical shift indicates a bridging carbonyl, and the ^{195}Pt satellite intensities indicate a triply bridging CO.[5]

The reaction of $P(OMe)_3$ with **2** occurred rapidly to give the adduct $[Pt_3\{P(OMe)_3\}(ReO_3)(\mu\text{-dppm})_3]^+$, **4**, as indicated by a color change from red−brown to red. The equilibrium constant for formation of **4** was favorable, but neither $P(OPh)_3$ or PPh_3 reacted with **2**, presumably due to steric hindrance. In forming **4**, the phosphite adds as a terminal ligand as shown by the NMR spectra in CD_2Cl_2 at −90 °C but the complex is fluxional.

The ^{31}P NMR spectra of **4** are very informative, and the spectra, in the $P(OMe)_3$ region only, at −90 and 22 °C are shown in Figure 2. At −90 °C, the resonance due to $P(OMe)_3$ is at $\delta = 188.2$ and appeared as a 1:4:1 triplet (due to coupling to Pt^1, $^1J(PtP) = 3713$ Hz) of 1:8:18:8:1 quintets (due to coupling to Pt^2 and Pt^3, $^2J(PtP) = 121$ Hz). This pattern is characteristic of the Pt_3 cluster containing a terminal phosphite ligand.[6] At 20 °C, this resonance appears as a 1:4:7:4:1 quintet due to apparently equal coupling to the three platinum atoms with observed coupling $^1J(PtP) = 1318$ Hz.[6] Evidently, the phosphite ligand migrates rapidly around the Pt_3 triangle and should then give an average value of $J(PtP) = (1/3 \times 3713) + (2/3 \times 121) = 1318$ Hz, in excellent agreement with the observed value of 1318 Hz. Since the coupling $J(PtP)$ is still observed in the region of fast fluxionality, the process cannot involve reversible dissociation of the phosphite ligand, but probably involves an intermediate with a triply bridging phosphite ligand. In the dppm region, only one resonance was observed at room temperature, but this splits into three resonances at −90 °C, consistent with the proposed structure and mechanism of fluxionality. Details are given in the Experimental Section. This fluxional process is similar to that established earlier in the complex $[Pt_3(\mu_3\text{-}CO)(\mu\text{-dppm})_3\{P(OMe)_3\}]^{2+}$.[6]

The monocation $[Pt_3(\mu_3\text{-}H)(\mu\text{-dppm})_3]^+$ reacts with the electrophiles H^+ and $AuPPh_3^+$ to give $[Pt_3(\mu_3\text{-}H)_2(\mu\text{-dppm})_3]^+$ and $[Pt_3(\mu_3\text{-}H)(\mu_3\text{-}AuPPh_3)(\mu\text{-dppm})_3]^+$, respectively,[7] and attempts were made to add these electrophiles to **2**. However, no reaction was observed. Since neither electrophile is bulky, the low reactivity of **2** is presumed to be due to electronic effects. In particular, the $\mu_3\text{-}ReO_3$ group in **2** is more electron withdrawing than μ_3-H, and so the Pt_3 center in **2** is not sufficiently electron rich to add electrophiles.

Reactions with Tl(I) and Hg(0). The complex thallium(I) acetyl acetonate [Tl(acac)] reacts readily with the cluster **5** to form the adduct $[Pt_3\{\mu_3\text{-}Tl(acac)\}(ReO_3)(\mu\text{-dppm})_3]^+$, **5**, by adding to the Pt_3 fragment as shown in eq 3. The reaction took

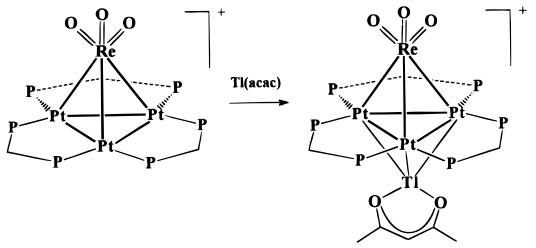

(3)

ca. 0.5 h to reach completion as monitored by NMR spectroscopy, and the sparingly soluble [Tl(acac)] dissolved as the reaction proceeded in acetone. Well-shaped red−black crystals of the stable cluster **5** can be obtained from acetone/hexane solution. There are few complexes containing platinum−thallium bonds, two recent examples being $[Pt_3(\mu_3\text{-}Tl)(\mu\text{-}CO)_3(PCy_3)_3][Rh(\eta\text{-}C_8H_{12})Cl_2]$ (Cy = cyclohexyl),[8] which also contains a $Pt_3(\mu_3\text{-}Tl)$ unit, and $(Bu_4N)_2[PtTl(C_6F_5)_4]$,[9] which contains thallium(II).

Complex **5** was characterized spectroscopically. The IR spectrum gave two terminal oxo bands at $\nu(Re{=}O) = 932$ and 901 cm^{-1}. The values of $\nu(ReO)$ in **5** are slightly higher than those in **2**, suggesting that Tl(acac) acts as a weak acceptor (it can be considered as a 2-electron donor ligand using the $6s^2$

(4) Ferguson, G.; Lloyd, B. R.; Puddephatt, R. J. *Organometallics* **1986**, *5*, 344.
(5) Puddephatt, R. J.; Manojlović-Muir, L.; Muir, K. W. *Polyhedron* **1990**, *9*, 2767.
(6) Bradford, A. M.; Douglas, G.; Manojlović-Muir, L.; Muir, K. W.; Puddephatt, R. J. *Organometallics* **1990**, *9*, 409.
(7) (a) Payne, N. C.; Ramachandran, R.; Schoettel, G.; Vittal, J. J.; Puddephatt, R. J. *Inorg. Chem.* **1991**, *30*, 4048. (b) Ramachandran, R.; Puddephatt, R. J. *Inorg. Chem.* **1993**, *32*, 2256.
(8) Ezomo, O. J.; Mingos, D. M. P.; Williams, I. D. *J. Chem. Soc., Chem. Commun.* **1987**, 924.
(9) Uson, R.; Fornies, J.; Tomas, M.; Garde, R.; Alonso, P. J. *J. Am. Chem. Soc.* **1995**, *117*, 1837.

Scheme 1

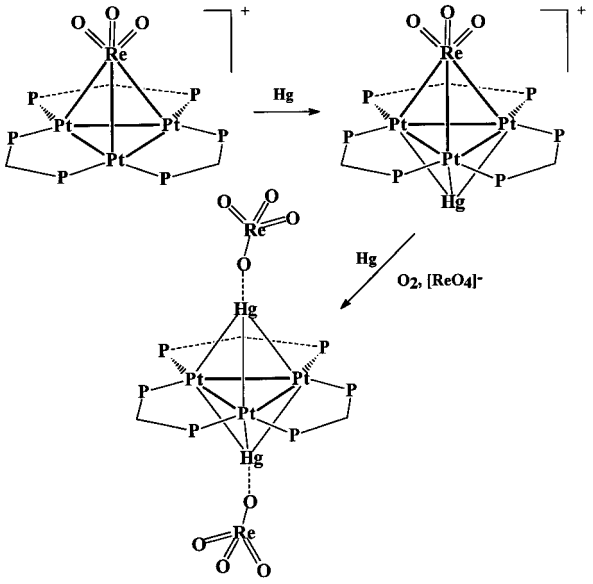

electrons). The ^{31}P NMR spectrum of **5** contains a single dppm resonance which appears as a 1:1 doublet due to coupling to thallium, and the magnitude of ^2J(TlP) = 180 Hz for **5** is comparable to that of ^2J(TlP) = 193 Hz found in the closely related cluster $[Pt_3(\mu_3\text{-Tl})(\mu\text{-CO})_3(PCy_3)_3][Rh(\eta\text{-}C_8H_{12})Cl_2]$ whose structure was determined by X-ray diffraction.[8] Thus, effective 3-fold symmetry is established, indicating easy rotation of the Tl(acac) unit with respect to the Pt_3 triangle. The values of ^1J(PtP) = 3212 and ^3J(PP) = 133 Hz in **5** are slightly higher and lower, respectively, than those of cluster **2**, indicating slightly weaker Pt−Pt bonding in the $Pt_3(\mu\text{-dppm})_3$ triangle in **5**. The ^{1}H NMR spectrum of **5** contained two resonances for the $P_2CH^aH^b$ protons at $\delta(^1H)$ = 6.17 and 5.92 and two acac resonances at $\delta(^1H)$ = 5.64 and 2.28 in a 1:6 ratio, corresponding to the CH and Me protons, respectively, fully consistent with the proposed structure.

Similarly, mercury reacts with cluster **2** at room temperature to form the new adduct $[Pt_3(ReO_3)(\mu_3\text{-Hg})(\mu\text{-dppm})_3][PF_6]$, **6**, as shown in Scheme 1. The reaction was complete in 30 min, as indicated by a color change to red and as monitored by ^{1}H and ^{31}P NMR spectroscopy. Cluster **6** is stable in acetone solution in the presence of excess mercury for at least 2 months. Well-shaped red−black cubic crystals of cluster **6** were obtained from an acetone/hexane solution. The reaction to form **6** is analogous to that of mercury with $[Pt_3(\mu_3\text{-CO})(\mu\text{-dppm})_3][PF_6]_2$ to form $[Pt_3(\mu_3\text{-CO})(\mu_3\text{-Hg})(\mu\text{-dppm})_3]^{2+}$,[10] but this reaction is reversible whereas the formation of **6** is not. Cluster **6**, in the presence of free mercury and perrhenate ion, is oxidized in the presence of O_2 to give $[Pt_3(\mu_3\text{-Hg})_2(\mu\text{-dppm})_3][ReO_4]_2$, **7**, (Scheme 1). The dimercury cluster **7** was previously prepared as the $[PF_6]^-$ salt by reaction of $[Pt_3(\mu_3\text{-CO})(\mu_3\text{-Hg})(\mu\text{-dppm})_3]^{2+}$ with mercury in the presence of Me_3NO.[10] Of several known platinum−mercury-bonded complexes,[11] the closest analogies to **7** are found in the dimercury-capped clusters, with the $Pt_3(\mu_3\text{-Hg})_2$ core $[Pt_3(\mu_3\text{-HgX})_2(\mu\text{-CO})_3L_3]$ (X = Cl, Br, I; L = PCy_3, $PPhCy_2$, PPh^iPr_2, P^iPr_3), of which the cluster with X = Br and L = $PPhCy_2$ was characterized structurally.[12]

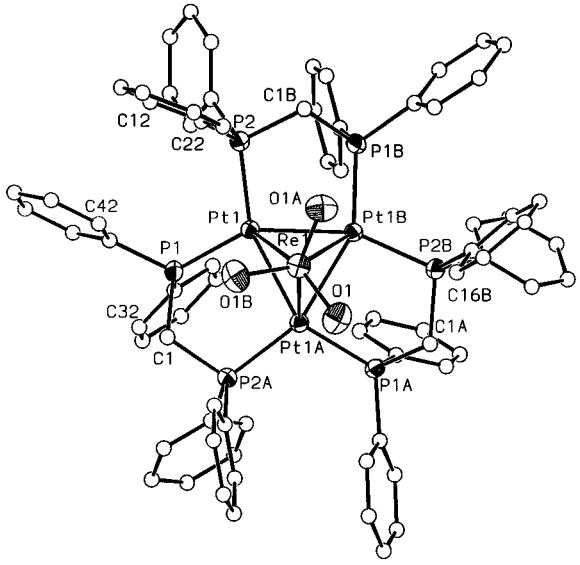

Figure 3. A view of the structure of $[Pt_3(ReO_3)(\mu\text{-dppm})_3]^+$. The carbon atoms are represented by spheres of arbitrary radius, and the remaining non-hydrogen atoms, by 30% probability ellipsoids. Hydrogen atoms are omitted for clarity. Phenyl carbon atoms are numbered in sequence C*n*1−C*n*6, where *n* = 1−4, starting with the *ipso* atom, and labels are shown only for the C*n*2 atoms. Symmetry operations applied are (A) *z*, *x*, *y* and (B) *y*, *z*, *x*.

The IR spectrum of **6** displayed three terminal oxo bands at ν(Re═O) = 943 (s), 913 (s), and 907 (s) cm^{-1}, the frequencies being slightly higher than those in cluster **5**. As expected, the ^{31}P NMR spectrum of **6** contained a singlet resonance due to the six equivalent phosphorus atoms of the dppm ligands, and the ^{1}H NMR spectrum contained two resonances in a 1:1 ratio for the $CH^aH^bP_2$ protons, showing that there is no plane symmetry containing the $Pt_3P_6C_3$ atoms of the $Pt_3(\mu\text{-dppm})_3$ unit.

The IR spectrum of **7** displays two very strong bands at ν(ReO) = 896 and 866 cm^{-1} due to the coordinated $[ReO_4]^-$ ions. The ^{31}P NMR spectrum contained a singlet resonance due to the dppm phosphorus atoms, and the ^{1}H NMR spectrum contained only one resonance due to the CH_2P_2 protons of the dppm ligands, indicating D_{3h} symmetry in this case.

The Structures of 2[PF$_6$], 6[PF$_6$], and 7[ReO$_4$]$_2$. The structure of the cation $[Pt_3(ReO_3)(\mu\text{-dppm})_3]^+$, **2**, was first determined as the $[ReO_4]^-$ salt, despite the poor quality of the crystals.[1b] Now crystals of **2**$[PF_6]$ have been obtained, which are of higher quality and have cubic symmetry. Given the importance of **2** in the chemistry described above, it was considered worthwhile to determine the structure with a classic noncoordinating anion.

The structure of **2** as found in the $[PF_6]^-$ salt is shown in Figure 3 and is characterized by the bond lengths and angles listed in Table 1. It contains a triangular Pt_3 unit edge bridged by three dppm ligands, yielding the well-known latitudinal $Pt_3(\mu\text{-dppm})_3$ moiety.[5] The Pt_3 triangle is capped by a ReO_3 group

(10) Schoettel, G.; Vittal, J. J.; Puddephatt, R. J. *J. Am. Chem. Soc.* **1990**, *112*, 6400.

(11) (a) Imhof, D.; Venanzi, L. M. *Chem. Soc. Rev.* **1994**, 185. (b) Gade, L. H. *Angew. Chem., Int. Ed. Engl*. **1993**, *32*, 24. (c) Yamamoto, Y.; Yamazaki, H.; Sakurai, T. *J. Am. Chem. Soc.* **1982**, *104*, 2329. (d) Yamamoto, Y.; Yamazaki, H. *J. Chem. Soc., Dalton Trans.* **1989**, 2161. (e) Yamamoto, Y.; Yamazaki, H. *Inorg. Chim. Acta* **1994**, *217*, 121. (f) Mingos, D. M. P.; Wardle, R. W. M. *J. Chem. Soc., Dalton Trans.* **1986**, 73. (g) Bour, J. J.; Vanderberg, W.; Schlebos, P. P. J.; Kanters, R. P. F.; Schoondergang, M. F. J.; Bosman, W. P.; Smits, J. M. M.; Beurskens, P. T.; Steggerda, J. J.; Vandersluis, P. *Inorg. Chem.* **1990**, *29*, 2971. (h) Ito, L. N.; Felicissimo, A. M. P.; Pignolet, L. H. *Inorg. Chem.* **1991**, *30*, 387. (i) Carlson, T. F.; Fackler, J. P.; Staples, R. J.; Winpenny, R. E. P. *Inorg. Chem.* **1995**, *34*, 426. (j) Toronto, D. V.; Balch, A. L. *Inorg. Chem.* **1994**, *33*, 6132. (k) Wurst, K.; Strahle, J. *Z. Anorg. Allgem. Chem.* **1991**, *595*, 239. (l) Tanase, T.; Horiuchi, T.; Yamamoto, Y. *J. Organomet. Chem.* **1992**, *440*, 1. (m) Albinati. A.; Moor, A.; Pregosin, P. S.; Venanzi, L. M. *J. Am. Chem. Soc.* **1982**, *104*, 7672.

(12) Albinati, A.; Dahmen, K.-H.; Demartin, F.; Forward, J. M.; Longley, C. J.; Mingos, D. M. P.; Venanzi, L. M. *Inorg. Chem.* **1992**, *31*, 2223.

Table 1. Selected Bond Lengths (Å) and Angles (deg) for $[Pt_3(ReO_3)(Ph_2PCH_2PPh_2)_3]^+$ [a]

Pt(1)−P(2)	2.275(2)	P(1)−C(31)	1.834(6)
Pt(1)−P(1)	2.294(2)	P(1)−C(1)	1.838(10)
Pt(1)−Pt(1A)	2.6115(6)	P(2)−C(21)	1.823(6)
Pt(1)−Re(1)	2.7010(6)	P(2)−C(11)	1.846(6)
Re(1)−O(1)	1.705(8)	P(2)−C(1B)	1.840(10)
P(1)−C(41)	1.824(6)		

P(2)−Pt(1)−P(1)	112.47(9)	C(41)−P(1)−C(31)	106.4(4)
P(2)−Pt(1)−Pt(1A)	157.75(7)	C(41)−P(1)−C(1)	101.7(4)
P(1)−Pt(1)−Pt(1A)	89.75(6)	C(31)−P(1)−C(1)	104.3(4)
P(2)−Pt(1)−Pt(1B)	98.12(7)	C(41)−P(1)−Pt(1)	120.7(3)
P(1)−Pt(1)−Pt(1B)	146.87(6)	C(31)−P(1)−Pt(1)	112.7(2)
P(2)−Pt(1)−Re(1)	106.41(7)	C(1)−P(1)−Pt(1)	109.3(3)
P(1)−Pt(1)−Re(1)	118.16(6)	C(21)−P(2)−C(11)	103.0(4)
Pt(1A)−Pt(1)−Re(1)	61.09(1)	C(21)−P(2)−C(1B)	103.9(4)
O(1)−Re(1)−O(1A)	108.4(3)	C(11)−P(2)−C(1B)	102.5(4)
O(1)−Re(1)−Pt(1B)	101.7(3)	C(21)−P(2)−Pt(1)	120.9(3)
O(1)−Re(1)−Pt(1A)	83.7(3)	C(11)−P(2)−Pt(1)	114.8(3)
Pt(1A)−Re(1)−Pt(B)	57.82(2)	C(1B)−P(2)−Pt(1)	109.7(3)
O(1)−Re(1)−Pt(1)	141.4(3)		

[a] Symmetry transformations used to generate equivalent atoms: (A) *z*, *x*, *y*, (B) *y*, *z*, *x*.

to form a distorted tetrahedral Pt_3Re core. The structure shows exact, crystallographically imposed C_3 symmetry, the 3-fold axis passing through the rhenium atom and the center of the Pt_3 triangle.

In the Pt_3ReO_3 unit the rhenium atom has distorted octahedral geometry [O−Re−O 108.4(3)°, Pt−Re−O 83.7(3), 101.7(3), and 141.4(3)°]. Each Re−O bond is directed toward a P1 and away from a P2 atom (Figure 3), and the Pt_3O_3 octahedron is, therefore, distorted toward trigonal prismatic geometry, with a twist angle of 20.3°. This distortion, also apparent from Figure 4a, may be caused by weak attractive interactions involving the polar oxo groups of the ReO_3 unit and the hydrogen atoms of the phenyl substituents in the $Pt_3(\mu\text{-dppm})_3$ fragment, resulting in three short intramolecular O···H distances [O(1)···H(C16B) 2.39(1) Å]. A similar trigonal twist of the coordination octahedron around the rhenium center has been found in the closely related structure of **1**, in which the oxo groups of **2** are replaced by carbonyl groups.[1c]

The structures of the Pt_3ReO_3 units in **2**$[PF_6]$ and in **2**$[ReO_4]$ are essentially the same, but there are differences in the conformations of the $Pt_3(\mu\text{-dppm})_3$ fragments as a result of the different sizes and electronic properties of the anions. In **2**$[PF_6]$, all Pt−P bonds are bent out of the Pt_3 plane, the three Pt−P(2) bonds in the direction toward and the three Pt−P(1) bonds away from the ReO_3 group. The displacements of the P(2), C(1), and P(1) atoms from the Pt_3 plane are 0.169(3), 0.403(10), and −0.562(2) Å. Each Pt_2P_2C unit adopts an envelope conformation with a P(1) atom at the "flap". In such a conformation of the $Pt_3P_6C_3$ skeleton, all six phenyl substituents on the side of the P(2) atoms are equatorial and form a cavity large enough to accommodate the ReO_3 group, while the six axial phenyl groups completely encase the opposite side of the Pt_3 triangle (Figure 4). In the $[ReO_4]^-$ salt there is a different conformation which results in cavities above both faces of the Pt_3 triangle (Figure 4).[1b] The three Pt_2P_2C units again adopt envelope conformations but with CH_2 groups at the flaps, two on one side and one on the other side of the Pt_3 triangle. In this conformation of the $Pt_3P_6C_3$ unit, there are two axial and four equatorial phenyl substituents on one side of the Pt_3 plane, creating a cavity for the ReO_3 group, and four axial and two equatorial phenyl groups on the other side, creating a cavity for the $[ReO_4]^-$ anion (Figure 4). We have previously observed the ability of the $M_3(\mu\text{-dppm})_3$ unit to loosely bind an anion.[2,5,13] For example, in $[Pd_3(\mu_3\text{-CO})(\mu\text{-}CF_3CO_2)(\mu\text{-dppm})_3][CF_3CO_2]$[13b] and in $[Pt_3\{\mu_3\text{-Re}(CO)_3\}(\mu_3\text{-I})(\mu\text{-dppm})_3]$,[2b] the Pd−O and Re−I distances of 2.77(1)−2.92(2) and 3.113(1)−3.341(1) Å, respectively, are considered indicative of some degree of covalency. In **2**$[ReO_4]$, however, the shortest Pt−O distances [3.37(3), 3.41(3), and 3.98(3) Å] are too long to indicate a covalent-bonding interaction,[1b] and the binding is best considered to be of the host−guest type reminiscent of molecular recognition in organic compounds. In **2**$[PF_6]$ the conformation of the μ-dppm ligands precludes any association of cation and anion.

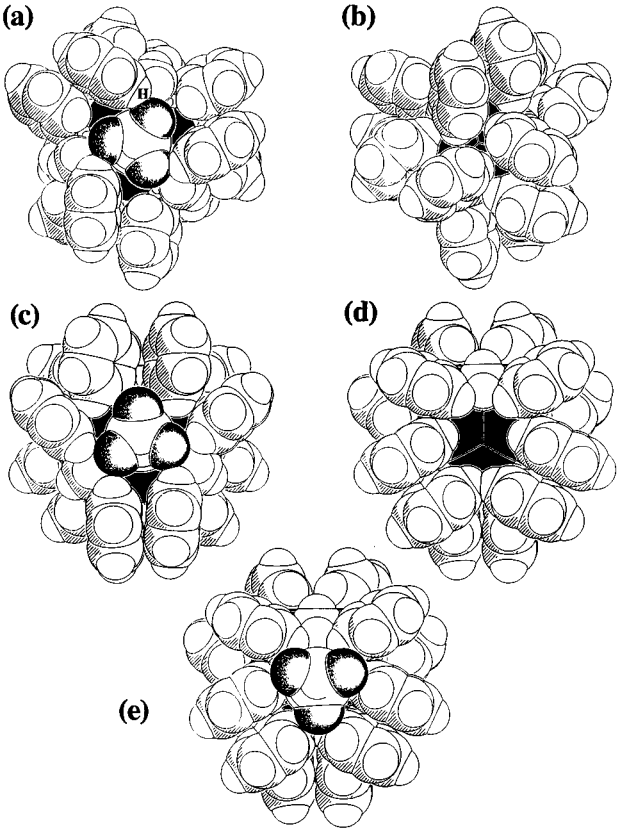

Figure 4. Space-filling diagrams for the $[Pt_3(ReO_3)(\mu\text{-dppm})_3]^+$ cation: (a, b) in the $[PF_6]^-$ salt; (c, d) in the $[ReO_4]^-$ salt. The platinum atoms are shown in black, and the oxygen atoms are dotted. In (a) and (b) the cation is viewed along the crystallographically imposed triad axis. The ReO_3 group points toward the viewer in (a) [H(16) is labeled H] and (c), and in (b) and (d), where it points away from the viewer, it is obscured. In (e) the $[ReO_4]^-$ anion is also displayed, lying enclosed in the cavity shown in (d).

The Pt−Pt distances in **2**$[PF_6]$ of 2.6115(6) Å are indicative of single bonds and are comparable with those in **2**$[ReO_4]$ of 2.598(2)−2.609(3) Å[1b] and in **1** of 2.5930(9)−2.6114(7) Å,[1c] all of which are among the shortest known in $Pt_3(\mu\text{-dppm})_3$ derivatives.[1−7] The Pt−Re bonds in **2**$[PF_6]$ of 2.7010(6) Å are longer than those in **1** [2.6488(8)−2.6850(8) Å].[1c] Thus, replacement of a $Re(CO)_3$ group in **1** by the ReO_3 group in **2** does not affect the Pt−Pt bonds but leads to somewhat longer Pt−Re bonds. The Pt−Re bonds in **2** are longer in the $[ReO_4]^-$ salt [2.711(3), 2.720(3), and 2.748(3) Å][1b] than those in the $[PF_6]^-$ salt [2.7010(6) Å]. This can be understood in terms of the relative cavity sizes for the $Pt_3(ReO_3)$ groups as discussed earlier (Figure 4, parts a and c). In **2**$[PF_6]$ the O−Re−O angles

(13) (a) Lloyd, B. R.; Manojlović-Muir, L.; Muir, K. W.; Puddephatt, R. J. *Organometallics* **1993**, *12*, 1231. (b) Ferguson, G.; Lloyd, B. R.; Manojlovic-Muir, L.; Muir, K. W.; Puddephatt, R. J. *Inorg. Chem.* **1986**, *25*, 4190. (c) Manojlović-Muir, L.; Muir, K. W.; Lloyd, B. R.; Puddephatt, R. J. *J. Chem. Soc., Chem. Commun.* **1985**, 536. (d) Manojlović-Muir, L.; Muir, K. W.; Lloyd, B. R.; Puddephatt, R. J. *J. Chem. Soc., Chem. Commun.* **1983**, 1336.

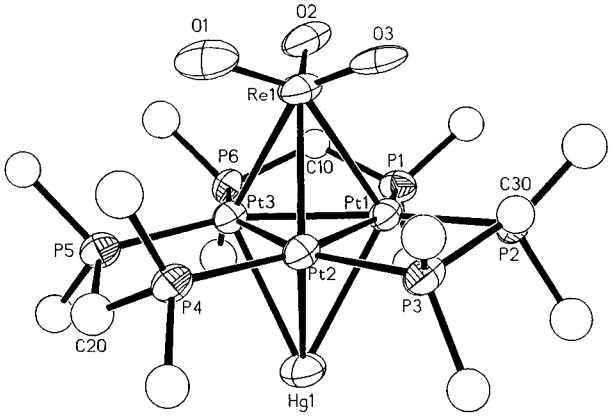

Figure 5. A view of the structure of $[Pt_3(ReO_3)(Hg)(\mu\text{-dppm})_3]^+$. Carbon and oxygen atoms and Re(2) are shown as spheres of arbitrary radius while other non-hydrogen atoms are shown as 50% probability ellipsoids. Only one orientation of the disordered $[ReO_4]^-$ ions is shown.

are 108.4(3)°, considerably larger than the C−Re−C angles of 88.2(5)−91.0(5)° in **1**, and the Re−O distances within the ReO_3 group of 1.705(8) Å are within the known range of those found in compounds containing the ReO_3 group (1.66−1.77 Å).[14] The lengthening of the Pt−P(1) bonds [2.294(2) Å] with respect to the Pt−P(2) bonds [2.275(2) Å] in **2**[PF_6] may be caused by steric congestion above the face of the Pt_3 triangle where all six phenyl groups are axial (Figure 4b).

The structure of **6**, as found in the $[PF_6]^-$ salt, is shown in Figure 5, and bond distances and angles are in Table 2. The cluster cation **6** contains a distorted trigonal bipyramidal Pt_3-ReHg metal core. There is a Pt_3 triangle with each edge bridged by a μ-dppm ligand, and with one face capped by the ReO_3 group and the other by a mercury atom. The three platinum atoms consist of an essentially equilateral triangle, with Pt−Pt distances of 2.617(2), 2.622(2), and 2.625(2) Å. The mean Pt−Pt distance of 2.621 Å in **6** is only slightly longer than that in **2** (2.6115 Å), indicating that addition of the μ_3-Hg group has little effect on the Pt−Pt bonding.[23] The Pt−Hg distances of 2.868(2)−2.976(2) Å with a mean value of 2.905 Å in **6** are similar to those of 2.860(2)−2.974(2) Å found in $[Pt_3(\mu_3\text{-Hg})(\mu_3\text{-CO})(\mu\text{-dppm})_3]^+$ and comparable to those in other clusters containing a $Pt_3(\mu_3\text{-Hg})$ unit.[10−12] The mean Pt−Re distance of 2.780 Å is longer than that of 2.702 Å in **2**. This could be due to the *trans* influence of the mercury atom or due to steric effects as discussed for **2**[ReO_4]. The Re−O distances of 1.637(2)−1.714(2) with a mean value of 1.687 Å are slightly shorter than those in **2** (1.705 Å), and the O−Re−O angles of 107(1)−109(1)° are indistinguishable from those in **2**. In this case, the shortest nonbonding H···O═Re distance is 2.50 Å, which is longer than that in **2**. The conformation of the dppm ligands is similar to that in **2**[ReO_4]; the Pt−P distances are normal and in the range of 2.274(1)−2.310(1) Å with a mean value of 2.294 Å.

The structure of **7** is shown in Figures 6 and 7, and bond distances and angles are in Table 3. The inner core of **7** contains a slightly distorted trigonal bipyramid of metal atoms Pt_3Hg_2 with both faces of the Pt_3 triangle capped by μ_3-Hg atoms (Figure 6), and the mercury atoms are weakly coordinated to the $[ReO_4]^-$ anions. By repeating this $[Pt_3(\mu_3\text{-Hg})_2(\mu\text{-dppm})_3][ReO_4]_2$ unit, a cluster polymer is formed as shown in Figure 7. The Hg−O distances are in the range of 2.39(4)−2.87(4) Å. All can be considered weak by comparison to the Pauling covalent Hg−O distance of 2.22 Å and the observed Hg−O distances of 2.21(3)−2.28(3) Å in the cluster $[HOs_5Hg_2(CO)_{15}(O_2CCF_3)_3]$.[15a] They are comparable to the weak Hg−O bonds found in $[Hg_3(\mu\text{-dppm})_3][SO_4]_2$ [2.54(2)−3.25(2) Å].[15b] Two of the Hg−O bond distances, Hg(2)−O(5) = 2.39(4) Å and Hg(2)−O(7A) = 2.56(4) Å, are shorter than the other two, Hg-

Table 2. Selected Bond Lengths (Å) and Angles (deg) for **6**

Hg(1)−Pt(1)	2.976(2)	Hg(1)−Pt(2)	2.868(2)
Hg(1)−Pt(3)	2.871(2)	Pt(1)−Pt(2)	2.625(2)
Pt(1)−Pt(3)	2.617(2)	Pt(2)−Pt(3)	2.622(2)
Pt(1)−Re(1)	2.788(2)	Pt(2)−Re(1)	2.781(2)
Pt(3)−Re(1)	2.770(2)	Pt(1)−P(1)	2.310(7)
Pt(1)−P(2)	2.274(8)	Pt(2)−P(3)	2.299(8)
Pt(2)−P(4)	2.297(8)	Pt(3)−P(5)	2.300(8)
Pt(3)−P(6)	2.283(7)	Re(1)−O(1)	1.71(2)
Re(1)−O(2)	1.71(2)	Re(1)−O(3)	1.64(3)
Pt(1)−Hg(1)−Pt(2)	53.4(1)	Pt(1)−Hg(1)−Pt(3)	53.1(1)
Pt(2)−Hg(1)−Pt(3)	54.4(1)	Hg(1)−Pt(1)−Pt(2)	61.2(1)
Hg(1)−Pt(1)−Pt(3)	61.4(1)	Pt(2)−Pt(1)−Pt(3)	60.0(1)
Hg(1)−Pt(1)−Re(1)	113.1(1)	Pt(2)−Pt(1)−Re(1)	61.7(1)
Pt(3)−Pt(1)−Re(1)	61.6(1)	Hg(1)−Pt(2)−Pt(1)	65.4(1)
Hg(1)−Pt(2)−Pt(3)	62.9(1)	Pt(1)−Pt(2)−Pt(3)	59.8(1)
Hg(1)−Pt(2)−Re(1)	116.7(1)	Pt(1)−Pt(2)−Re(1)	62.0(1)
Pt(3)−Pt(2)−Re(1)	61.6(1)	Hg(1)−Pt(3)−Pt(1)	65.5(1)
Hg(1)−Pt(3)−Pt(2)	62.8(1)	Pt(1)−Pt(3)−Pt(2)	60.2(1)
Hg(1)−Pt(3)−Re(1)	116.9(1)	Pt(1)−Pt(3)−Re(1)	62.2(1)
Pt(2)−Pt(3)−Re(1)	62.0(1)	Pt(1)−Re(1)−Pt(2)	56.3(1)
Pt(1)−Re(1)−Pt(3)	56.2(1)	Pt(2)−Re(1)−Pt(3)	56.4(1)
Pt(2)−Pt(1)−P(1)	155.6(2)	Pt(3)−Pt(1)−P(1)	95.7(2)
Pt(2)−Pt(1)−P(2)	96.0(2)	Pt(3)−Pt(1)−P(2)	156.0(2)
P(1)−Pt(1)−P(2)	108.3(3)	Pt(1)−Pt(2)−P(3)	94.7(2)
Pt(3)−Pt(2)−P(3)	154.5(2)	Pt(1)−Pt(2)−P(4)	154.9(2)
Pt(3)−Pt(2)−P(4)	95.2(2)	P(3)−Pt(2)−P(4)	110.2(3)
Pt(1)−Pt(3)−P(5)	155.2(2)	Pt(2)−Pt(3)−P(5)	96.1(2)
Pt(1)−Pt(3)−P(6)	95.6(2)	Pt(2)−Pt(3)−P(6)	155.8(2)
P(5)−Pt(3)−P(6)	108.0(3)	Pt(1)−Re(1)−O(1)	145.0(6)
Pt(2)−Re(1)−O(1)	94.5(6)	Pt(3)−Re(1)−O(1)	92.8(6)
Pt(1)−Re(1)−O(2)	90.6(5)	Pt(2)−Re(1)−O(2)	142.6(5)
Pt(3)−Re(1)−O(2)	92.3(6)	O(1)−Re(1)−O(2)	108.0(9)
Pt(1)−Re(1)−O(3)	93.8(6)	Pt(2)−Re(1)−O(3)	91.6(6)
Pt(3)−Re(1)−O(3)	144.0(6)	O(1)−Re(1)−O(3)	107.0(10)
O(2)−Re(1)−O(3)	108.9(10)		

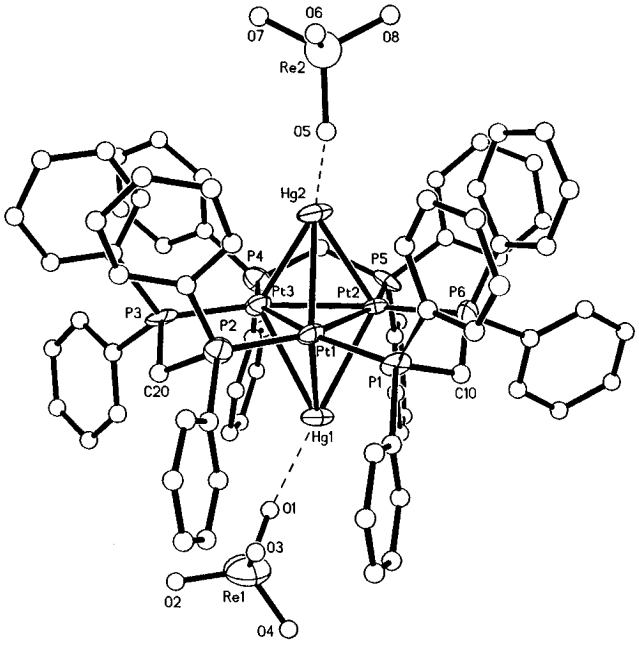

Figure 6. A view of the structure of $[Pt_3(Hg)_2(\mu\text{-dppm})_3][ReO_4]_2$. Carbon atoms are shown as spheres of arbitrary radius while other non-hydrogen atoms are shown as 50% probability ellipsoids. Only the *ipso* carbon aoms of the phenyl groups are shown for clarity.

(14) For example: (a) Domingos, A.; Marcalo, J.; Paulo, A.; Pires de Matos, A.; Santos, I. *Inorg. Chem.* **1993**, *32*, 5114. (b) Dignan, I. A.; Herrmann, W. A.; Herdtweck, E. *Chem. Ber.* **1990**, *123*, 1347. (c) Herrmann, W. A.; Kuchler, J. G.; Felixberger, J. K.; Herdtweck, E.; Wagner, W. *Angew. Chem., Int. Ed. Engl.* **1988**, *27*, 394.

Table 3. Selected Bond Distances (Å) and Angles (deg) for **7**[a]

Hg(1)−Pt(1)	2.754(4)	Hg(1)−Pt(2)	2.788(10)
Hg(1)−Pt(3)	2.828(4)	Hg(2)−Pt(3)	2.770(8)
Hg(2)−Pt(2)	2.773(4)	Hg(2)−Pt(1)	2.796(7)
Pt(1)−Pt(2)	2.646(4)	Pt(1)−Pt(3)	2.635(3)
Pt(2)−Pt(3)	2.633(4)	Pt(1)−P(1)	2.255(14)
Pt(1)−P(2)	2.27(2)	Pt(2)−P(6)	2.27(2)
Pt(2)−P(5)	2.30(2)	Pt(3)−P(3)	2.27(2)
Pt(3)−P(4)	2.28(2)	Hg(1)···O(1)	2.70(4)
Hg(1)···O(4)	2.87(4)	Hg(2)−O(5)	2.39(4)
Hg(2)O(7A)	2.56(4)		

Pt(1)−Hg(1)−Pt(2)	57.02(12)	Pt(1)−Hg(1)−Pt(3)	56.32(10)
Pt(2)−Hg(1)−Pt(3)	55.91(10)	Pt(3)−Hg(2)−Pt(2)	56.72(9)
Pt(3)−Hg(2)−Pt(1)	56.5(2)	Pt(2)−Hg(2)−Pt(1)	56.74(9)
Pt(2)−Pt(3)−Pt(1)	60.30(9)	Pt(3)−Pt(1)−Pt(2)	59.80(10)
Pt(3)−Pt(2)−Pt(1)	59.90(11)	Pt(3)−Pt(1)−Hg(1)	63.24(9)
Pt(3)−Pt(2)−Hg(1)	62.8(2)	Pt(1)−Pt(2)−Hg(1)	60.84(12)
Hg(2)−Pt(2)−Hg(1)	113.95(12)	Pt(2)−Pt(1)−Hg(1)	62.1(2)
Pt(3)−Pt(1)−Hg(2)	61.25(13)	Pt(2)−Pt(1)−Hg(2)	61.19(12)
Hg(1)−Pt(1)−Hg(2)	114.3(2)	Pt(3)−Pt(2)−Hg(2)	61.6(2)
Pt(1)−Pt(2)−Hg(2)	62.07(14)	Pt(2)−Pt(3)−Hg(2)	61.7(2)
Pt(1)−Pt(3)−Hg(2)	62.23(10)	Pt(2)−Pt(3)−Hg(1)	61.3(2)
Pt(1)−Pt(3)−Hg(1)	60.43(10)	Hg(2)−Pt(3)−Hg(1)	112.80(14)
O(5)−Hg(2)−Pt(1)	116.0(10)	O(7A)−Hg(2)−Pt(1)	175(2)
O(5)−Hg(2)−O(7A)#1	67.5(14)	O(5)−Hg(2)−Pt(3)	156.0(10)
O(7A)#1-Hg(2)−Pt(3)	118.9(14)	O(5)−Hg(2)−Pt(2)	142.3(10)
O(7A)#1-Hg(2)−Pt(2)	122.7(12)	P(1)−Pt(1)−P(2)	110.9(5)
P(1)−Pt(1)−Pt(3)	153.7(4)	P(2)−Pt(1)−Pt(3)	94.4(4)
P(1)−Pt(1)−Pt(2)	94.6(4)	P(2)−Pt(1)−Pt(2)	154.2(4)
P(6)−Pt(2)−P(5)	109.9(6)	P(6)−Pt(2)−Pt(3)	154.3(4)
P(5)−Pt(2)−Pt(3)	95.6(4)	P(6)−Pt(2)−Pt(1)	94.6(4)
P(5)−Pt(2)−Pt(1)	155.5(4)	P(3)−Pt(3)−P(4)	108.9(6)
P(3)−Pt(3)−Pt(2)	156.5(4)	P(4)−Pt(3)−Pt(2)	94.5(4)
P(3)−Pt(3)−Pt(1)	96.3(4)	P(4)−Pt(3)−Pt(1)	154.8(4)

[a] Symmetry transformations used to generate equivalent atoms: #1 $-x+1, -y+1, -z+2$.

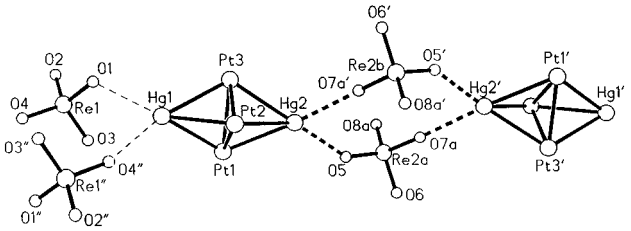

Figure 7. A view of part of the chain structure of $[Pt_3(Hg)_2(\mu\text{-dppm})_3][ReO_4]_2$. The dppm ligands are omitted, and only one orientation of each $[ReO_4]^-$ group is shown for clarity.

(1)−O(1) = 2.70(4) Å and Hg(1)−O(4) = 2.87(4) Å. The mean Pt−Pt distance in **7** (2.638 Å) is longer than that in **2** or **6**, while the Pt−Hg distances are in the range of 2.754(4)−2.828(4) Å with a mean distance of 2.785 Å and so are shorter than those in **6** (mean 2.905 Å). A structure which is closely related to **7** has been found in the cluster $[Pt_3(\mu\text{-CO})_3(PPhCy_2)_3(\mu_3\text{-}HgBr)_2]$ in which two trigonal bipyramidal Pt_3Hg_2 units are held together by two μ-Br bridging ligands.[12]

Discussion

The contrast between the Pt_3Re clusters **1** and **2** in terms of the selectivity and reactivity toward ligand addition is dramatic. Thus, CO and $P(OR)_3$ react with cluster **1** by addition to rhenium giving $[Pt_3\{Re(CO)_3L\}(\mu\text{-dppm})_3]^+$, L = CO or $P(OR)_3$, but react with **2** at platinum to give $[Pt_3(ReO_3)L(\mu\text{-dppm})_3]^+$, L = μ_3-CO (**3**) or $P(OR)_3$ (**4**). The addition to **2** appears to be more sensitive to steric effects than the addition to **1**, since $P(OR)_3$ reacts with **1** when R = Me or Ph but with **2** only when R = Me. The structure of **3** is analogous to those of $[Pt_3(\mu_3\text{-}SnX_3)(\mu_3\text{-CO})(\mu\text{-dppm})_3]^+$ (X = Cl or F)[16,17] and $[Pt_3(\mu_3\text{-Hg})(\mu_3\text{-CO})(\mu\text{-dppm})_3]^{2+}$.[10]

The reagents Tl^+ or Hg fail to react with **1** but add to **2** to give the isoelectronic clusters $[Pt_3(\mu_3\text{-}ReO_3)(\mu_3\text{-Tl})(\mu\text{-dppm})_3]^{2+}$, **5**, or $[Pt_3(\mu_3\text{-}ReO_3)(\mu_3\text{-Hg})(\mu\text{-dppm})_3]^+$, **6**, respectively, each of which contain three different metals. In each case, the main group metal is considered to bind to the Pt_3ReO_3 cluster by donation of its $6s^2$ electron pair to vacant p_z orbitals on each platinum atom with back-bonding from platinum into the vacant 6p orbitals of Tl^+ or Hg(0). According to EHMO calculations on the model clusters $[Pt_3(ReO_3)(Hg)(\mu\text{-}H_2PCH_2PH_2)_3]^+$ and $[Pt_3(Hg)_2(\mu\text{-}H_2PCH_2PH_2)_3]^+$, the charge on each mercury atom is −0.19 e in **6** and −0.18 e in **7**, and so it seems that mercury is a (weak) net acceptor ligand in these complexes. However, the calculated charge on thallium in $[Pt_3(ReO_3)(Tl)(\mu\text{-}H_2PCH_2PH_2)_3]^{2+}$ is +1.20 e, indicating that Tl^+ is a weak net donor ligand. However, it should be noted that the values of ν(Re=O) are higher in both **5** and **6** compared to those in **2**, consistent with both Hg(0) and Tl(I) being acceptors and thus increasing ReO π-bonding in **5** and **6**. Of course, as well as considering complexes **5** and **6** as adducts of **2** with the 2-electron ligands Tl(acac) and Hg(0), respectively, it is also valid to consider them as pentanuclear trimetallic clusters with Pt_3ReTl and Pt_3ReHg cores. The easy formation of these unusual clusters emphasizes the remarkable acceptor properties of the coordinatively unsaturated cluster **2**.

Experimental Section

The compounds $[Pt_3(\mu_3\text{-H})(\mu\text{-dppm})_3][PF_6]$,[14] $[MeReO_3]$,[15] and $[Pt_3\{ReO_3\}(\mu\text{-dppm})_3][PF_6]$[3c] were prepared according to the previously reported procedures.

$[Pt_3(\mu_3\text{-CO})\{ReO_3\}(\mu\text{-dppm})_3][PF_6]$ (3). To a solution of **2**$[PF_6]$ (28 mg, 0.013 mmol) in CD_2Cl_2 (0.5 mL) in an NMR tube was bubbled CO for 10 s. Immediately, the red−brown solution became lighter to give a clear red solution. The product **3** was characterized spectroscopically by NMR and IR in solution since removal of the solvent afforded only the starting material **2**$[PF_6]$. IR (CH_2Cl_2): ν(CO) = 1606 (m) cm^{-1}, ν(Re=O) of ReO_3 = 904 (m) cm^{-1}. NMR (CD_2Cl_2): ^{1}H, δ = 5.75 (m, 3H, H^aCP_2), 5.15 (m, 3H, H^bCP_2); $^{31}P\{^1H\}$, δ = −7.6 [s, 6P, ^1J(PtP) = 3507 Hz, ^2J(PtP) = −5 Hz, ^3J(PP) = 155 Hz, dppm]; $^{31}P\{^1H\}$ at −90 °C, δ = −6.4 [s, 6P, ^1J(PtP) = 3530 Hz, ^2J(PtP) = −6 Hz, ^3J(PP) = 150 Hz, dppm]. ^{1}H and ^{31}P NMR for the ^{13}CO-enriched sample in CD_2Cl_2 at room temperature gave spectral data that are the same as those above: $^{13}C\{^1H\}$, δ = 224.6 [quin, 1C, ^1J(PtC) = 513 Hz, μ_3-*C*O].

$[Pt_3\{P(OMe)_3\}\{ReO_3\}(\mu\text{-dppm})_3][PF_6]$ (4). To a solution of **2**$[PF_6]$ (30 mg, 0.014 mmol) in CD_2Cl_2 (0.5 mL) in an NMR tube was added trimethyl phosphite (1.7 μL, 1 equiv) via microsyringe at −78 °C. NMR spectra were recorded from −80 to 20 °C. Attempts to grow crystals of **4** from CH_2Cl_2/diethyl ether or acetone/hexane afforded mixtures of well-shaped black crystals, which were identified as the starting complex **2**$[PF_6]$ by ^{1}H and ^{31}P NMR and IR measurement, and orange−yellow crystals of **4**$[PF_6]$, whose quality was not suitable for X-ray crystallography. Anal. Calcd for $C_{78}H_{75}F_6O_6P_8Pt_3Re\cdot 2(CH_3)_2CO$: C, 42.79; H, 3.72. Found: C, 42.86; H, 3.73. IR (Nujol): ν(Re=O) of ReO_3 = 938 (s), 879 (s, br) cm^{-1}. NMR (CD_2Cl_2): ^{1}H, δ = 4.96 [br, 3H, H^aCP_2], 4.77 [br, 3H, H^bCP_2]; $^{31}P\{^1H\}$, δ = 186.7 [quin, br, 1P, ^1J(PtP) = 1318 Hz, $P(OMe)_3$], −14.5 [s, br, 6P, ^1J(PtP) = 2842 Hz, ^3J(PP) = 206 Hz, dppm]; ^{1}H at −80 °C, δ = 5.54 [br, 2H, H^aCP_2], 5.33 [br, 2H, H^bCP_2], 3.67 [m, 9H, $P(OMe)_3$], 3.39 [m, 1H, $H^{a'}CP_2$], 3.34 [m, 1H, $H^{b'}CP_2$]; $^{31}P\{^1H\}$ at −80 °C, δ = 188.2 [s, $2P^x$, ^1J(PtP) = 3713 Hz, ^2J(PtP) = 121 Hz, $P(OMe)_3$], −7.7 [s, $2P^b$, ^1J(PtP^b) =

(15) (a) Diebold, M. P.; Johnson, B. F. G.; Lewis, J.; Saharan, V. P.; McPartlin, M.; Powell, H. R. *J. Organomet. Chem.* **1991**, *405*, C25. (b) Hammerle, B.; Muller, E. P.; Wilkinson, D. L.; Muller, G.; Peringer, P. *J. Chem. Soc., Chem. Commun.* **1989**, 1527.

(16) (a) Douglas, G.; Jennings, M. C.; Manojlović-Muir, L.; Muir, K. W.; Puddephatt, R. J. *J. Chem. Soc., Chem. Commun.* **1989**, 159. (b) Jennings, M. C.; Schoettel, G.; Roy, S.; Puddephatt, R. J.; Douglas, G.; Manojlović-Muir, L.; Muir, K. W. *Organometallics* **1991**, *10*, 580.

(17) Lindsey, R. V., Jr.; Parshall, G. W.; Stolberg, U. G. *Inorg. Chem.* **1966**, *5*, 109.

2587 Hz, $^3J(P^bP^b)$ = 203 Hz, dppm], −8.0 [dm, 2P^a, $^1J(PtP^a)$ = 3504 Hz, $^3J(P^aP^c)$ = 196 Hz, dppm], −33.1 [dm, 2P^c, $^1J(PtP^c)$ = 2192 Hz, $^3J(P^aP^c)$ = 196 Hz, dppm].

The reaction of **2**[PF_6] with triphenyl phosphite or triphenylphosphine was studied in a similar manner as above. No reaction occurred at temperatures between −90 and 20 °C, according to ^{1}H and ^{31}P NMR measurements.

[Pt$_3$(μ_3-TlC$_5$H$_7$O$_2$){ReO$_3$}(μ-dppm)$_3$][PF_6] (5). To a solution of **2**[PF_6] (36 mg, 0.017 mmol) in acetone (15 mL) was added thallium acetyl acetonate (5.0 mg, 0.017 mmol). The orange suspension gradually became a clear red solution in 5 min. After 0.5 h of stirring, the solution was concentrated to ca. 2 mL. Hexane was added to precipitate the complex to give the product as orange−yellow crystals. Yield: 83%. Well-shaped red−black multifaced crystals can be obtained from acetone/hexane by the diffusion method. Anal. Calcd for $C_{80}H_{73}F_6O_5P_7Pt_3ReTl$: C, 39.69; H, 3.04. Found: C, 41.16; H, 3.09. IR (Nujol): ν(Re═O) of {ReO_3} = 932 (s), 901 (vs) cm^{-1}. NMR (CD_2Cl_2): ^{1}H, δ = 6.17 [br, 3H, H^aCP_2], 5.92 [br, 3H, H^bCP_2], 5.64 [br, 1H, CH($CH_3CO)_2$)], 2.28 [br, 6H, CH(CH_3CO)$_2$)]; ^{31}P{^{1}H}, δ = −3.0 [d, 6P, ^1J(PtP) = 3212 Hz, ^2J(TlP) = 180 Hz, ^3J(PP) = 147 Hz, dppm].

[Pt$_3$(μ_3-Hg){ReO$_3$}(μ-dppm)$_3$][PF_6] (6). To a solution of **2**[PF_6] (34 mg, 0.016 mmol) in acetone (15 mL) was added a drop of mercury by pipet. The orange suspension gradually became clear intense red in color. After 1 h of stirring, the unreacted mercury was removed. The solution was concentrated to ca. 2 mL. Hexane was added to precipitate the product as reddish-black crystals. Yield: 93%. Well-shaped black cubelike crystals were obtained from acetone/hexane. Anal. Calcd for $C_{75}H_{66}F_6O_3P_7HgPt_3Re\cdot 2(CH_3)_2CO$: C, 39.96; H, 3.73. Found: C, 39.75; H, 3.34. IR (Nujol): ν(Re═O) of ReO_3 = 943 (s), 913 (s, sh), 907 (s) cm^{-1}. NMR (CD_2Cl_2): ^{1}H, δ = 5.78 [br, 3H, H^aCP_2], 5.66 [br, 3H, H^bCP_2]; ^{31}P{^{1}H}, δ = −4.6 [s, 6P, ^1J(PtP) = 3151 Hz, ^2J(HgP) = 177 Hz, ^3J(PP) = 160 Hz, dppm].

[Pt$_3$(μ_3-Hg)$_2$(μ-dppm)$_3${ReO$_4$}$_2$] (7). To a solution of **2**[PF_6] (30 mg, 0.014 mmol) in CH_2Cl_2 (15 mL) was added a drop of mercury by pipet. After 0.5 h of stirring, the dark brown solution gradually became clear red. At this stage, complex **6** was formed. Ammonium perrhenate (4.0 mg, 0.014 mmol) was then added to this solution. After 12 h of stirring while exposed to air, an orange solution was formed which was concentrated and precipitated by hexane to give the product as golden brown crystals. Well-shaped black−red rectangular crystals can be obtained from an acetone solution of **7**. Yield: 86%. Anal. Calcd for $C_{75}H_{66}F_6Hg_2O_8P_6Pt_3Re_2\cdot 1.5(CH_3)_2CO$: C, 35.01; H, 2.77. Found: C, 36.08; H, 2.84. IR (Nujol): ν(Re═O) of $[ReO_4]^-$ = 896 (s), 866 (s) cm^{-1}. NMR (CD_2Cl_2): ^{1}H, δ = 5.75 [s, 6H, H_2CP_2]; ^{31}P-{^{1}H}, δ = −5.1 [s, 6P, ^1J(PtP) = 3143 Hz, ^2J(HgP) = 187 Hz, ^3J(PP) = 173 Hz, dppm].

Reaction with H$^+$. To a solution of cluster **2** (32 mg, 0.015 mmol) in CD_2Cl_2 in an NMR tube was added excess trifluoroacetic acid. No reaction took place as monitored by spectroscopic methods. The cluster **2** is even unreactive to hydrochloric acid.

Reaction with AuPPh$_3^+$. A solution of [Au(THF)PPh_3][PF_6], which was freshly prepared from [AuCl(PPh_3)] (17 mg, 0.033 mmol) in THF (10 mL) and $AgPF_6$ (9 mg, 0.033 mmol) and then filtered, was added dropwise to a solution of **2** (35 mg, 0.017 mmol) in THF (10 mL) while stirring. No reaction occurred in solution during a period of 2 days or after evaporation of the solution as indicated by NMR spectroscopy.

X-ray Crystal Structure Analyses. A summary of the crystal data and analyses is given in Table 4. Measurements for **2**[PF_6] were made by using an Enraf-Nonius CAD4 diffractometer and for **6**[PF_6] and **7**[ReO_4]$_2$, with crystals in flame-sealed capillary tubes to prevent solvent loss, using a Siemens P4 diffractometer, with graphite-monochromated Mo Kα radiation in all cases.

2[PF_6]. The unit cell dimensions were determined from the diffractometric angles for 25 reflections with 20.8 ≤ 2θ(Mo Kα) ≤ 24.7°. The intensities of reflections were measured by $\omega/2\theta$ scans, with scan speeds adjusted to give $\sigma(I)/I$ < 0.03, subject to a time limit of 30 s. Three reflections were measured every 2 h in order to monitor stability of the crystal and diffractometer. The intensities were corrected for Lorentz, polarization, crystal decomposition (6.8% intensity loss over 200 h), and absorption effects. The absorption correction was applied using the ψ-scan method[18] (correction factor on F^2 was 0.409−0.999, corresponding to a difference in mean transmission path of 0.12 mm). Of 12 962 reflections measured, only 3900 (R_{int} = 0.088) were symmetrically independent and were used in the structure analysis.

Table 4. Crystal Data and Experimental Details for **2**[PF_6], **6**[PF_6]·2Me_2CO, and **7**[ReO_4]$_2$·1.5Me_2CO

formula	$C_{75}H_{66}F_6O_3P_7Pt_3Re$	$C_{81}H_{78}F_6HgO_5P_7Pt_3Re$	$C_{79.5}H_{75}Hg_2O_{9.5}Pt_3Re_2$
fw	2117.54	2434.35	2727.06
cryst. sys.	cubic	triclinic	triclinic
space group	$Pa\bar{3}$ (No. 205)	$P\bar{1}$	$P\bar{1}$
a, Å	24.495(1)	14.502(5)	16.088(5)
b, Å		16.712(7)	16.307(7)
c, Å		20.814(6)	19.390(7)
α, deg		70.00(3)	99.49(2)
β, deg		82.52(1)	93.70(1)
γ, deg		82.39(3)	117.30(2)
V, Å^3	14697(1)	4679(3)	4401(4)
Z	8	2	2
d (calcd), g cm^{-3}	1.914	1.727	2.058
temp, °C	20	25	25
λ, Å	0.71073	0.71073	0.71073
abs coeff, mm^{-1}	7.549	7.57	11.12
F(000)	8064	2304	2524
reflns[a]	3113	7227	3946
parameters	250	356	363
R	0.0421	0.0688	0.1010
R_w	0.0883[c]	0.0711[b]	0.2149[c]

[a] $I > 2\sigma(I)$, $R = \sum(|F_o| - |F_c|)/\sum|F_o|$. [b] $R_w = [\sum w(|F_o| - |F_c|)^2/\sum w|F_o|^2]^{1/2}$. [c] $wR_2 = [\sum w(F_o^2 - F_c^2)^2/\sum w|F_o|^4]^{1/2}$.

The structure was solved by the heavy atom method[19] and refined to convergence by full-matrix least-squares method on F^2, with $w = 1/[\sigma^2(F^2) + (0.0375P)^2 + 137P]$, where $P = [F_{obs}^2 + 2F_{calc}^2]/3$. All non-hydrogen atoms were assigned anisotropic displacement parameters. Hydrogen atoms were allowed to ride on the parent carbon atoms, with C−H distances of 0.93 Å in C_6H_5 and 0.97 Å in CH_2 groups and with isotropic displacement parameters U(H) = 1.2U_{eq}(C). Neutral atom scattering factors and anomalous dispersion corrections were taken from ref 20. All refinement calculations were performed using the SHELX-93 program package.[21]

The final atomic parameters are listed in Table 5. The unit cell contains eight cations, each with crystallographic symmetry 3 and with its Re(1) atom lying exactly on the triad axis (Wykoff site *c*). Four of the eight $[PF_6]^-$ anions present in the unit cell are accounted for by the atoms P(3) (on Wykoff site *a*) and F(3) which defines a $[PF_6]^-$ anion with exact 3 symmetry. The remaining four anions, defined by the atoms P(4), F(4A), and F(4B) (all with site occupancy factors of 1/2), have 3-fold symmetry [P(4) on Wykoff site *c*] and are disordered over eight equivalent sites. All the fluorine atoms, and also to a lesser extent the carbon atoms C(44), C(45), and C(46), have displacement parameters whose size (see Table 3) and anisotropy are suggestive of disorder. Attempts to model this disorder were not successful.

6[PF_6]. The cell constants were obtained by centering 25 high-angle reflections (14.0 ≤ 2θ ≤ 24.9°).[22] The Laue symmetry $\bar{1}$ was determined by merging symmetry equivalent reflections. During data collection three standards were monitored for every 297 data measured. The data were collected in the 2θ range of 4.0−46° (−1 ≤ h ≤ 15, −17 ≤ k ≤ 17, −22 ≤ l ≤ 22) in ω scan mode at variable scan speeds (1−10 deg/min). Background measurements were made at the ends of the scan range. The data processing, solution, and refinements were done using *SHELXTL-PC* programs.[23] The data were corrected for

(18) MOLEN, Crystallographic Program Package, Enraf-Nonius, Delft, The Netherlands, 1991.
(19) Sheldrick, G. M. SHELXS86, Program for Solution of Crystal Structures, University of Goettingen, Germany, 1985.
(20) *International Tables for X-ray Crystallography*; *International Union of Crystallography*; Kluwer: Dordrecht, The Netherlands, 1992; Vol. C.
(21) Sheldrick, G. M. SHELX93, Program for Refinement of Crystal Structures, University of Goettingen, Germany, 1993.
(22) XSCANS, Siemens Analytical X-Ray Instruments Inc., Madison, WI, 1990.

Table 5. Atomic Fractional Coordinates ($\times 10^4$) and Displacement Parameters ($\times 10^3$ Å^2) for $[Pt_3(ReO_3)(Ph_2PCH_2PPh_2)_3][PF_6]$

atom	*x*	*y*	*z*	U_{eq}[a]
Pt(1)	2076(1)	2305(1)	1463(1)	38(1)
Re(1)	2476(1)	2476(1)	2476(1)	53(1)
P(1)	1415(1)	2887(1)	1145(1)	45(1)
P(2)	2810(1)	2257(1)	0896(1)	45(1)
P(3)	1/2	1/2	0	41(1)
P(4)	9396(3)	4396(3)	604(3)	58(3)
F(3)	4862(14)	4910(9)	0561(7)	312(12)
F(4A)	9301(11)	4531(17)	166(13)	248(20)
F(4B)	9630(16)	4287(12)	1055(11)	205(13)
O(1)	2312(4)	2393(4)	3147(3)	83(3)
C(1)	1132(4)	3278(4)	1719(4)	53(3)
C(11)	3251(3)	2868(2)	0897(3)	57(3)
C(12)	3242(3)	3220(3)	0457(3)	80(4)
C(13)	3563(4)	3683(3)	0460(3)	93(4)
C(14)	3893(4)	3794(3)	0903(4)	96(5)
C(15)	3902(3)	3442(4)	1343(3)	94(4)
C(16)	3581(3)	2979(3)	1340(3)	78(4)
C(21)	2724(3)	2113(3)	0171(2)	54(3)
C(22)	2203(3)	2090(3)	−0041(3)	68(3)
C(23)	2125(4)	1968(4)	−0586(3)	98(5)
C(24)	2569(5)	1867(3)	−0918(2)	107(6)
C(25)	3090(4)	1890(3)	−0706(3)	101(5)
C(26)	3168(3)	2013(3)	−0161(4)	78(4)
C(31)	0826(3)	2525(3)	0858(3)	55(3)
C(32)	0329(3)	2774(3)	0767(3)	69(3)
C(33)	−0102(2)	2477(4)	0560(3)	91(5)
C(34)	−0036(3)	1929(4)	0443(3)	101(5)
C(35)	0461(4)	1680(3)	0534(4)	95(5)
C(36)	0892(3)	1978(3)	0742(3)	65(3)
C(41)	1586(3)	3428(3)	0662(3)	57(3)
C(42)	2017(3)	3768(3)	0789(3)	81(4)
C(43)	2168(4)	4175(3)	0431(4)	90(4)
C(44)	1889(5)	4243(4)	−0054(4)	150(9)
C(45)	1459(5)	3903(4)	−0181(3)	175(11)
C(46)	1307(4)	3495(4)	0177(3)	120(7)

[a] U_{eq} is one-third of the trace of the orthogonalized anisotropic displacement tensor.

absorption by the Gaussian method after indexing the faces of the data crystal and measuring the distances between the faces. The minimum and the maximum transmission factors are 0.2854 and 0.4776, respectively. Of 13 639 reflections collected, 12 363 were independent ($R = 0.0431$) and were used in the least-squares refinement. The structure was solved by direct methods followed by subsequent difference Fourier routines. Anisotropic thermal parameters were assigned and refined for Hg, Pt, Re, P, and O atoms. All the phenyl rings were treated as ideal hexagons with C−C distance of 1.395 Å. No attempt was made to locate the hydrogen atom positions, and all the hydrogen atoms in the cation were placed in the calculated positions, and they were included for the purpose of structure factor calculations only. A common thermal parameter was assigned for all hydrogen atoms and refined in the least-squares cycles. In the PF_6^- anion, the fluorine atoms in the equatorial positions were found to be disordered. Two different orientations of the disordered F atoms were found to be related by rotation of 45° around the F(1)−P(7)−F(2) axis, and their occupancies (0.55/0.45) were derived from the ratio of their electron densities obtained from the difference Fourier routines. Due to this disorder problem, each fragment was treated as an ideal octahedron and a common P−F distance was refined (to 1.488 Å) in the least-squares cycles. Common isotropic thermal parameters were assigned for each set of disordered fluorine atoms and refined. Four fragments of acetone solvent molecules located in the crystal lattice were added to two molecules. Ideal geometrical constraints were imposed (C−O = 1.20 Å, C−C = 1.54 Å, and C−C−C and C−C−O = 120°) for all the acetone fragments. Common isotropic thermal parameters were assigned for each set of acetone fragment and refined. Hydrogen atoms were not included for the solvent molecule. In the final full-matrix refinements on *F*, the model converged at $R = 0.0688$, $R_w = 0.0711$, $R_g = 0.0907$, and GOF = 1.43 for 7227 observations with $F_o \geq 4\sigma(F_o)$ and 356 parameters. The maximum shift/esd = −0.013 for rot(*z*) O(7). The electron density in the final difference Fourier synthesis fluctuates in the range from 1.66 to −2.16 e Å^{-3}. The top 10 peaks were associated with the heavy metal atoms. Inclusion of empirical absorption corrected data did not improve the refinement parameters. Atomic parameters are given in Table 6.

(23) Sheldrick, G. M. SHELXTL-PC Software, Siemens Analytical X-Ray Instruments Inc., Madison, WI, 1990.

Table 6. Selected Atomic Coordinates ($\times 10^4$) for **6**

atom	*x*	*y*	*z*
Hg(1)	2478.7(10)	3684.1(7)	1968.2(5)
Pt(1)	2399.2(8)	1833.0(6)	2208.8(4)
Pt(2)	1675.7(8)	2462.0(6)	3179.1(4)
Pt(3)	3492.9(1)	2273.5(6)	2911.7(4)
Re(1)	2577.5(9)	815.8(7)	3570.8(5)
P(1)	3588(5)	1420(4)	1501(3)
P(2)	1015(5)	1625(4)	1916(3)
P(3)	153(5)	2401(4)	3014(3)
P(4)	1721(5)	3076(4)	4006(3)
P(5)	3846(5)	2966(4)	3620(3)
P(6)	4857(5)	1906(4)	2353(3)
O(1)	2763(15)	810(11)	4369(8)
O(2)	3467(14)	178(11)	3316(9)
O(3)	1594(18)	395(12)	3652(9)
C(10)	4642(17)	1151(14)	1936(10)
C(20)	2827(19)	3598(16)	3854(12)
C(30)	71(18)	1592(14)	2633(11)

Table 7. Selected Atomic Coordinates ($\times 10^4$) for **7**

atom	*x*	*y*	*z*
Hg(1)	1830(2)	1548(2)	6319(1)
Hg(2)	3585(2)	3729(2)	8419(1)
Pt(1)	2248(2)	3227(2)	7220(1)
Pt(2)	2287(2)	1872(2)	7784(1)
Pt(3)	3651(2)	2826(2)	7098(1)
P(1)	796(10)	2926(11)	7462(8)
P(2)	2814(11)	4391(11)	6602(8)
P(3)	4418(10)	3894(11)	6441(8)
P(4)	4458(12)	2015(11)	7260(8)
P(5)	2896(12)	914(10)	8057(7)
P(6)	957(11)	1556(12)	8277(8)
Re(1)	1106(3)	875(2)	4326(2)
O(1)	1663(53)	632(56)	4982(36)
O(2)	1859(57)	1262(77)	3753(45)
O(3)	880(78)	1739(66)	4714(46)
O(4)	106(55)	−86(51)	3942(49)
O(2A)	1853(60)	1889(54)	4131(53)
O(3A)	223(64)	1013(86)	4678(48)
O(4A)	659(78)	−19(55)	3631(39)
Re(2)	4456(5)	5858(5)	10066(4)
Re(2A)	4672(5)	6125(5)	9817(4)
O(5)	3800(28)	5041(25)	9312(19)
O(6)	4190(29)	6778(26)	10149(21)
O(7)	5642(26)	6309(39)	10035(35)
O(8)	4205(52)	5363(40)	10778(25)
O(7A)	5101(45)	5830(40)	10552(26)
O(8A)	5531(39)	6650(39)	9374(33)
C(10)	210(39)	1821(36)	7690(28)
C(20)	3533(39)	4152(39)	5977(28)
C(30)	4174(38)	1518(38)	7988(28)

$7[ReO_4]_2$. Long rodlike red crystals were grown from acetone solution at room temperature. The crystals were examined under paraffin oil. The cell constants were obtained by centering 25 reflections ($21.4 \leq 2\theta \leq 24.8°$). The crystal diffracted weakly, and the ω scans were broad. Three standard reflections monitored at the end of every 297 data points collected showed steady decay of the crystal. The data collection was stopped at the end of shell $2\theta = 40°$ (the minimum and maximum decay correction factors are 0.734 and 1.000). A total of 8753 reflections were collected in the 2θ range of 4.0−40.0° ($-1 \leq h \leq 14$, $-15 \leq k \leq 13$, $-18 \leq l \leq 18$) in ω scan mode at variable scan speeds (2−10 deg/min). Background measurements were made at the ends of the scan range. An empirical absorption was applied to the data. The maximum and minimum transmission factors were 0.192 and 0.121, respectively. In the triclinic system, the

space group $P\bar{1}$ was assumed and the correctness of the choice of the space group was supported by the successful solution and refinement of the structure. The data processing, solution, and initial refinements were done using *SHELXTL-PC* programs.[23] The final refinements were performed using *SHELXL-93* software programs.[21] No attempt was made to locate the hydrogen atoms, but all hydrogen atoms were placed in calculated positions, and they were included for the purpose of structure factor calculations only. The isotropic thermal parameters of the hydrogen atoms were allowed to ride on the appropriate C atoms. Both of the ReO_4^- anions were found to be disordered. The oxygen atoms O(2), O(3), and O(4) were disordered (50:50) around Re(1) and were related by a rotation along Re(1)−O(1) bond. The disordered fragments of Re(2), O(7), and O(8) were related by a mirror plane containing O(5) and O(6) atoms. Isotropic thermal parameters were refined for the Re(2) and Re(2A) atoms. Due to the disorder problem, soft geometrical constraints were imposed (SADI) for Re−O and O···O distances. The common isotropic thermal parameter was refined for each set of oxygen atoms in the least-squares cycles. The difference Fourier routines indicated the presence of acetone solvate in three different positions. The site occupancies were 0.6, 0.4, and 0.5, as derived from the electron densities. One of the acetone fragments was disordered over two positions, with the fragments related by a mirror plane, with O(12) and C(19) in the mirror plane. Ideal constraints were imposed (DFIX, C−O = 1.20 Å and C−C = 1.54 Å) for these solvent molecules. Common isotropic thermal parameters were assigned for each set of fragments and refined. No H atoms were included for the disordered acetone molecule. All of the Hg, Pt, and P atoms, and the Re(1) atom, were refined anisotropically. In the final least-squares refinement cycles on F^2, the model converged at R1 = 0.101, wR2 = 0.215, and GOF = 1.01 for 3946 observations with $F_o \geq 4\sigma(F_o)$ and 363 parameters. In the final difference Fourier synthesis, the electron density fluctuated in the range from 2.51 to −3.12 e $Å^{-3}$. The top two peaks were found near Re(2A) and Re(2), respectively, and the next nine peaks were found around heavy metals Pt, Hg, and Re. The mean and the maximum shift/esd in the final cycles were 0.016 and 0.619. Atomic parameters are given in Table 7, and further details have been included in the supplementary materials.

Acknowledgment. We thank the NSERC (Canada), the EPSRC (UK), and the University of Glasgow for financial support and the Iranian Ministry of Science for a Studentship (to A.A.T.).

Supporting Information Available: Tables of crystal data, coordinates of all atoms, complete bond lengths and angles, anisotropic displacement parameters of non-hydrogen atoms, and calculated H-atom coordinates for **2[PF_6]**, **6**[PF_6], and **7**[ReO_4]$_2$ (Tables S1−S17) (30 pages). Ordering information is given on any current masthead page.

IC950825N